WATER RESOURCES RESEARCH, VOL. 37, NO. 1, PAGES 83–97, JANUARY 2001

Toward capturing hydrologically significant connectivity in spatial patterns

Andrew W. Western

Cooperative Research Centre for Catchment Hydrology and Centre for Environmental Applied Hydrology
Department of Civil and Environmental Engineering, University of Melbourne, Parkville, Victoria, Australia

Günter Blöschl

Institut für Hydraulik, Gewässerkunde und Wasserwirtschaft, Technische Universität Wien, Vienna, Austria

Rodger B. Grayson

Centre for Environmental Applied Hydrology and Cooperative Research Centre for Catchment Hydrology
Department of Civil and Environmental Engineering, University of Melbourne, Parkville, Victoria, Australia

Abstract. Many spatial fields exhibit connectivity features that have an important influence on hydrologic behavior. Examples include high-conductivity preferred flow paths in aquifers and saturated source areas in drainage lines. Connected features can be considered as arbitrarily shaped bands or pathways of connected pixels having similar (e.g., high) values. Connectivity is a property that is not captured by standard geostatistical approaches, which assume that spatial variation occurs in the most random possible way that is consistent with the spatial correlation, nor is it captured by indicator geostatistics. An alternative approach is to use connectivity functions. In this paper we apply connectivity functions to 13 observed soil moisture patterns from the Tarrawarra catchment and two synthetic aquifer conductivity patterns. It is shown that the connectivity functions are able to distinguish between connected and disconnected patterns. The importance of the connectivity in determining hydrologic behavior is explored using rainfall-runoff simulations and groundwater transport simulations. We propose the integral connectivity scale as a measure of the presence of hydrologic connectivity. Links between the connectivity functions and integral connectivity scale and simulated hydrologic behavior are demonstrated and explained from a hydrologic process perspective. Connectivity functions and the integral connectivity scale provide promising means for characterizing features that exist in observed spatial fields and that have an important influence on hydrologic behavior. Previously, this has not been possible within a statistical framework.

1. Introduction

Spatial variability is an intrinsic feature of natural hydrologic systems. The characteristics of that variability often have a substantial influence on the behavior of the system. Hydrologically important examples include soil moisture [*Western et al*., 1999], surface runoff [*Dunne et al*., 1975], and hydraulic conductivity in aquifer formations [*Anderson*, 1997]. From a scientific perspective, we need to understand the different characteristics present in spatial patterns to be able to understand system behavior more fully [*Koltermann and Gorelick*, 1996]. From a practical perspective we often need to know which are the important characteristics of a spatial pattern to make accurate predictions. For example, predictions related to processes such as erosion and salinization or estimates of the optimum siting of groundwater wells are inherently dependent on the spatial patterns of the underlying fields of hydrologically important features. The different characteristics of spatial patterns strongly influence flow paths. Therefore they become particularly important when we are interested in transport problems such as contaminant plume migration [*Anderson*, 1997].

Paper number 2000WR900241.
0043-1397/01/2000WR900241$09.00

Spatial patterns of hydrologic processes can exhibit a range of different characteristics, varying in a qualitative manner from random to highly organized [*Gutknecht*, 1993; *Blöschl et al*., 1993; *Blöschl and Grayson*, 2000]. Specific characteristics of a pattern can be defined quantitatively. Some patterns have no organization (white noise) or limited organization. Limited organization may be associated with spatial correlations and represents "continuity." The way the spatial correlation changes with distance between two points characterizes the degree of spatial continuity of the variable studied [*Journel and Huijbregts*, 1978, p. 13]. Correlations over large scales (i.e., large correlation lengths or integral correlation scales) are characteristic of smooth, highly continuous patterns, whereas patterns with large amounts of small-scale variability have little continuity, i.e., they change suddenly and the correlation lengths are small. We use the variogram and integral correlation scale as quantitative measures of continuity in this paper. Patterns with limited or no organization are referred to as random. Other patterns are more highly organized. Organized patterns can include connected features (i.e., connected thin bands such as high-conductivity flow paths) or convergent fea-

tures (i.e., a branching structure of drainage lines and hillslopes) [*Blöschl and Sivapalan*, 1995]. We focus on organization characterized by connected features in this paper.

Specifically, we will use the term "connectivity" to denote the extent to which connected features, such as arbitrarily shaped bands or pathways having similar (e.g., high) values, are present in a hydrologically relevant spatial pattern. We define connectivity quantitatively by using connectivity functions and the integral connectivity scale, which are described in detail in section 3.

It is possible for the characteristics of a pattern to change over time. For example, soil moisture patterns measured in the Tarrawarra catchment in southeastern Australia exhibit both continuity and connectivity during wet periods but only continuity during dry periods [*Grayson et al*., 1997; *Western et al*., 1998b; *Western et al*., 1999]. *Western et al*. [1998b] discuss spatial connectivity in greater detail. While there are well-developed techniques for characterizing random patterns, techniques for characterizing organized features of spatial patterns (such as connectivity) are less well developed and tested [*Koltermann and Gorelick*, 1996].

The proper representation of connectivity can be critically important for hydrologic prediction. For example, incorporating connectivity into antecedent moisture patterns has a dramatic effect on simulated runoff [*Bronstert and Bárdossy*, 1999; *Merz and Plate*, 1997; *Grayson et al*., 1995], even if the continuity (the spatial correlation structure or variogram) is unchanged [*Grayson et al*., 1995]. Similarly, simulation studies suggest that transport in groundwater systems is strongly influenced by the presence of connected bands of high hydraulic conductivity, which lead to preferred flow paths [*Desbarats and Srivastava*, 1991; *Sánchez-Vila et al*., 1996; *Gómez-Hernández and Wen*, 1997]. When moving from flow to transport problems, the actual flow paths become vastly more important [*Anderson*, 1997]. Thus it is essential to represent spatial variability in a way that captures the characteristics of the spatial patterns that are the most important influences on system response. This can either be done statistically or deterministically. In this paper we concentrate on characterizing connectivity within a statistical framework.

There is a range of geostatistical tools available for characterizing spatial patterns. Standard geostatistics (variogram analysis) only represents continuity and is therefore not able to distinguish between patterns with and without connectivity [*Grayson et al*., 1995; *Sánchez-Vila et al*., 1996; *Gómez-Hernández and Wen*, 1997]. It has been suggested that indicator geostatistics are an appropriate tool for characterizing connectivity [*Journel and Alabert*, 1988; *Anderson*, 1997]. In indicator geostatistics, variograms of indicator variables are compared for different thresholds, and a deviation from the expected difference in spatial correlation between the thresholds is sometimes taken as evidence of connectivity. Indicator variables are binary variables that represent the spatial pattern thresholded at different values. However, *Western et al*. [1998b] showed that indicator geostatistics could not distinguish between random and connected soil moisture patterns. They capture differences in continuity at different thresholds (which may be useful to know about) but not connectivity.

An alternative approach to capturing connectivity statistically is to use connectivity statistics. The concept of connectivity is most widely studied in the context of percolation [*Grimmet*, 1989; *Gould and Tobochnik*, 1988; *Stauffer and Aharony*, 1991]. It has been suggested by *Allard* [1994] for analyzing flow processes in petroleum reservoirs. Like indicator variograms, connectivity statistics also summarize patterns of indicator variables. However, they differ from indicator geostatistics in that they consider the probability that separate points with high indicator values are connected by any arbitrary continuous path of high values, whereas indicator variograms only consider the probability that two separate points have the same indicator value. Here we examine three questions: (1) How well do connectivity statistics distinguish between connected and random patterns, (2) can these connectivity statistics be related to differences in simulated hydrologic response, and (3) how important is the connectivity from a hydrological perspective? This is done using high-resolution measured spatial patterns of soil moisture from the Tarrawarra catchment [*Western and Grayson*, 1998] and synthetic patterns of aquifer conductivity. It should be noted that this paper is concerned with continuous patterns, so the connectivity of features like fracture networks (that often occur in rocks [*Clemo and Smith*, 1997; *Gavrilenko and Gueguen*, 1998]) will not be considered in this paper.

This paper is organized as follows. First, we provide a description of the Tarrawarra catchment and the soil moisture and aquifer patterns used in our analysis. Then we address connectivity statistics and their calculation, and we discuss the results obtained when they are applied to our data sets. Next we discuss surface runoff and groundwater transport simulations to explore how differences in connectivity are related to hydrologic response. Finally, we provide a discussion and conclusions.

2. Site and Data Description

We use two case studies in this paper. The first considers soil moisture patterns from the Tarrawarra catchment and the second a pair of hypothetical aquifers. Tarrawarra is a 10.5 ha catchment located in southeastern Australia [*Western and Grayson*, 1998]. The climate is temperate, and rainfall is spread relatively uniformly through the year. Potential evapotranspiration is high in summer and low in winter, which results in low soil moisture during summer and high soil moisture during winter. Depth average volumetric soil moisture in the top 30 cm of the soil profile was measured at points on a 10 by 20 m grid using time domain reflectometry on 13 occasions between September 1995 and November 1996. Each pattern consists of ~500 measurements. Figure 1 shows typical soil moisture patterns from this data set. In summer the average soil moisture is low and randomly distributed across the catchment (Figure 1a, survey S3). As the catchment becomes wetter during the autumn, relatively wet patches develop in the highly convergent upper parts of the drainage lines due to the influence of subsurface flow (Figure 1b, S5). In winter, average soil moisture is high and connected bands of relatively high soil moisture exist in the drainage lines (Figure 1c, S6). These wet bands are connected to the catchment outlet. Table 1 summarizes the soil moisture statistics of the 13 patterns. Further discussion of the seasonal change in the characteristics of the spatial patterns is provided by *Grayson et al*. [1997] and *Western et al*. [1999], while indicator patterns are presented by *Western et al*. [1998b]. Figure 2 shows variograms for the three soil moisture patterns in Figure 1. *Western et al*. [1998a] provide further analysis of the geostatistics of these patterns and analyze the seasonal changes in the spatial correlation of soil moisture. They found high variability and short correlation lengths during wet peri-

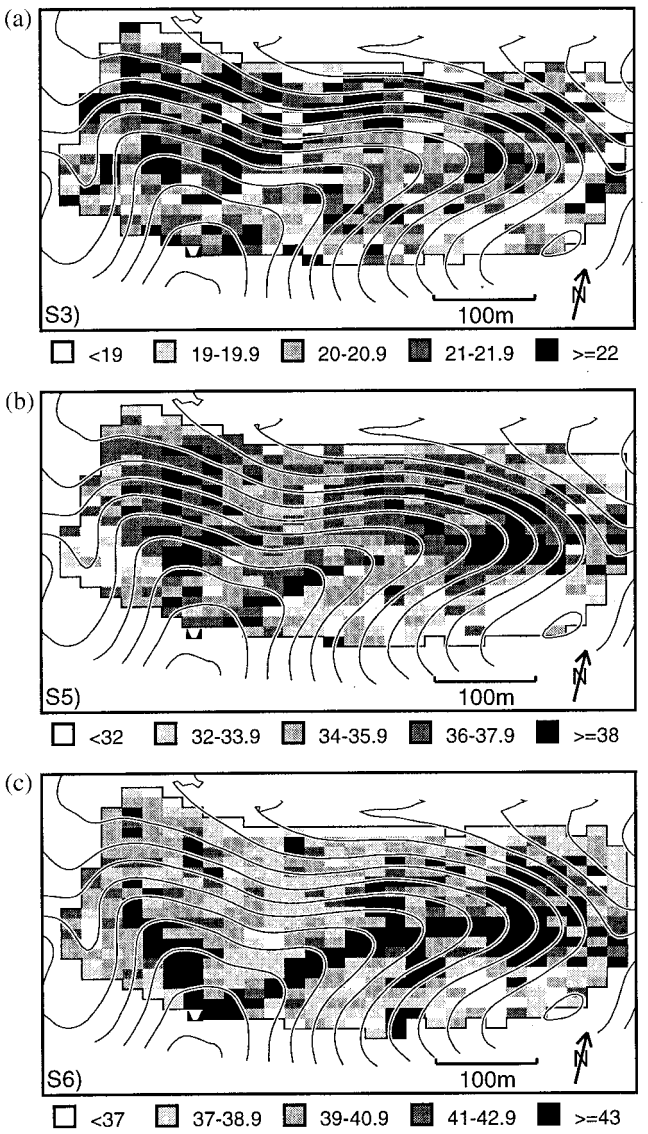

Figure 1. Soil moisture patterns from Tarrawarra showing different degrees of connectivity. (a) random soil moisture pattern February 23, 1996 (S3). (b) developing connectivity April 13, 1996 (S5). (c) connected soil moisture pattern April 22, 1996 (S6). Note that each pixel represents a point measurement of the volumetric soil moisture in the upper 30 cm of the soil profile. Contours show the surface topography; contour intervals are 2 m.

ods and low variability with longer correlation lengths during dry periods.

The second data set used in this paper consists of a pair of hypothetical two-dimensional aquifers [*Blöschl and Sivapalan*, 1995]. These patterns represent the distribution of hydrologic conductivities in space (map views) and consist of 256 × 384 pixels covering an area of 6000 × 9000 m. The first pattern has two sinusoidal high-conductivity preferential flow paths in a lower-conductivity medium (Figure 3). The mean conductivities for the high-conductivity channels and the low-conductivity medium are 10 and 0.1 mm/s, respectively, and the standard deviation of the log conductivity of the entire pattern is 1.9. This standard deviation appears to be typical of natural aquifers [*Gelhar*, 1993]. The second pattern is a random pattern generated using the turning bands method [*Mantoglou and Wilson*, 1981]. It has the same probability density function and variogram (Figure 4) as the first pattern but does not have any connected features. Both patterns are approximately isotropic, and both are approximately stationary. The pattern exhibiting the preferential flow paths was constructed to resemble realistic paleochannels as are sometimes observed in fluvial deposits [*Bierkens and Weerts*, 1994; *Scheibe and Freyberg*, 1995; *Kupfersberger and Blöschl*, 1995; *Koltermann and Gorelick*, 1996; *Anderson*, 1997]. It represents a scenario where the actual location of the sedimentary structure is known. The random pattern, on the other hand, represents a scenario where either no preferred channels are present or a scenario where these channels are present in nature but cannot be detected from the available data. If the aquifer in Figure 3a was sampled by a few point data (e.g., pumping tests) and the conductivities were interpolated by some sort of geostatistical simulation method (e.g., sequential Gaussian simulation [*Deutsch and Journel*, 1992]), one would typically obtain a random pattern similar to the one shown in Figure 3b.

3. Connectivity Measures

3.1. Methods

We use connectivity statistics [*Allard*, 1994] to characterize the connectivity of the spatial patterns. These connectivity statistics apply to indicator values Z, which are binary patterns obtained by thresholding the original pattern. $Z = 1$ if the original value is above the threshold, and $Z = 0$ otherwise. Let G be the set of pixels making up the spatial pattern, and let A be the set of pixels in G with $Z = 1$. Two pixels, x and x' in A, are connected (denoted by $x \leftrightarrow x'$) if there is a continuous path of neighboring pixels belonging to $A(x_1, \ldots, x_n \in A)$ between them (Figure 5). The connectivity function $\tau(h)$ represents the lag-dependent probability that a pixel (x) in A is connected to any pixel $(x + h)$ in G that is separated from x by the distance h. That is,

$$\tau(h) = P(x \leftrightarrow x + h | x \in A, x + h \in G). \quad (1)$$

Note that this definition is consistent with that usually used in percolation theory [*Stauffer and Aharony*, 1991; *Gould and Tobochnik*, 1988]. The connectivity function and the indicator variogram are similar in that they operate on indicator patterns; however, they quantify different characteristics of the patterns. The indicator variogram represents the lag-dependent variance between $Z(x)$ and $Z(x + h)$. This is related to the probability that $Z(x)$ and $Z(x + h)$ are the same. Specifically, the indicator variogram value is 1 minus the probability that $z(x)$ and $z(x + h)$ are the same. The difference between the two is that the indicator variogram does not consider whether x and $x + h$ are connected, whereas the connectivity function does. More detailed discussion of the connectivity approach is given by *Allard* [1994] and *Allard and Group* [1993] and in the percolation literature [*Grimmet*, 1989; *Gould and Tobochnik*, 1988; *Stauffer and Aharony*, 1991].

The behavior of connectivity functions (and related concepts, such as cluster size) has been extensively studied for random percolation processes in an infinite domain [*Grimmet*, 1989; *Stauffer and Aharony*, 1991]. When the proportion of high $(Z = 1)$ pixels is less than the critical percolation threshold, $\tau(h)$ decays approximately exponentially (equation (2)) [*Stauffer and Aharony*, 1991; *Grimmet*, 1989]. The percolation threshold is the threshold at which a cluster that spans the

Table 1. Summary of the 13 Soil Moisture Patterns From Tarrawarra[a]

Survey	Date	Pattern	Mean, % vol/vol	Variance, (% vol/vol)^2	Percentiles, % vol/vol			I_τ (Directional)			Integral Correlation Scale, m	75% Indicator Correlation Length, m
					50%	75%	90%	50%, m	75%, m	90%, m		
S1	Sept. 27, 1995	C	37.7	24.1	38.1	39.6	44.6	222	110	41	44	30
S2	Feb. 14, 1996	R	26.2	10.6	26.6	28.4	29.8	100	38	9	27	25
S3	Feb. 23, 1996	R	20.8	5.31	20.8	22.1	23.7	56	19	9	22	20
S4	Mar. 28, 1996	R	23.9	7.06	24.0	25.8	26.9	180	18	6	28	25
S5	Apr. 13, 1996	T	35.2	12.3	35.8	37.5	38.6	230	41	15	34	30
S6	Apr. 22, 1996	C	40.5	14.6	39.5	43.0	46.0	235	140	66	28	30
S7	May 2, 1996	C	41.4	19.4	40.4	45.0	46.8	232	123	57	34	30
S8	July 3, 1996	C	45.0	14.0	45.6	47.0	48.6	240	155	25	30	35
S9	Sept. 2, 1996	C	48.5	13.9	48.2	50.4	53.8	166	72	21	30	35
S10	Sept. 20, 1996	C	47.3	15.2	47.4	48.9	52.3	206	83	23	31	30
S11	Oct. 25, 1996	C	35.0	19.2	34.9	37.4	39.3	199	78	30	30	30
S12	Nov. 10, 1996	R	29.3	10.8	29.5	31.3	33.4	191	83	23	38	25
S13	Nov. 29, 1996	R	23.9	6.28	24.2	25.5	26.6	198	28	13	39	30

[a]All soil moisture values are expressed as percentages using a volumetric basis. C, connected; R, random; T, transition; as determined by visual inspection. Note that the integral connectivity scales I_τ are large for the connected patterns and small for the random patterns.

entire domain appears. For rectangular lattices, P_c is ~0.5–0.6. The exponential parameter ξ in (2) is called the percolation process correlation (or connectivity) length.

$$\tau(h) = e^{-h/\xi}. \tag{2}$$

For organized patterns, such as some of the Tarrawarra soil moisture patterns used in this paper, $\tau(h)$ no longer decays in an exponential manner. We propose here an integral connectivity scale I_τ, which we define in a similar manner to the integral correlation scale used in traditional geostatistics and fluid dynamics, which was originally introduced by *Taylor* [1921].

$$I_\tau = \int_0^\infty \tau(h)\, dh. \tag{3}$$

I_τ represents the average distance over which pixels are connected. For random fields that are fully characterized by their probability density function and their variogram the two integral scales are directly related. However, for fields that exhibit connectivity, this is no longer the case. For these fields, I_τ is large if significant connected bands are present, while I_τ is small if they are not (i.e., the random case). For a given integral correlation scale the integral connectivity scale I_τ will increase with the degree of connectivity present in the pattern.

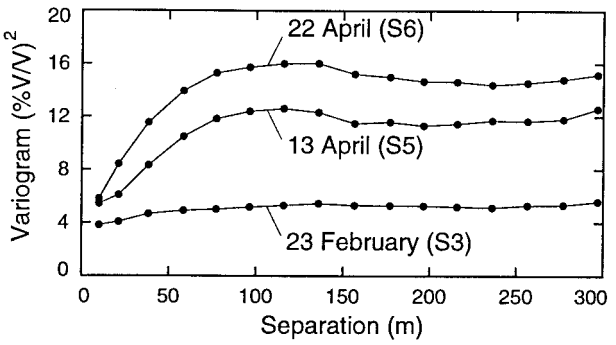

Figure 2. Variograms for the soil moisture patterns from Tarrawarra on February 23, 1996 (random), April 13, 1996 (developing connectivity), and April 22, 1996 (connected) (see Figure 1).

As is the case with variograms, it is possible to impose directional constraints on connectivity functions. In this paper we consider omnidirectional connectivity and topographically defined directional connectivity. Details of the computation

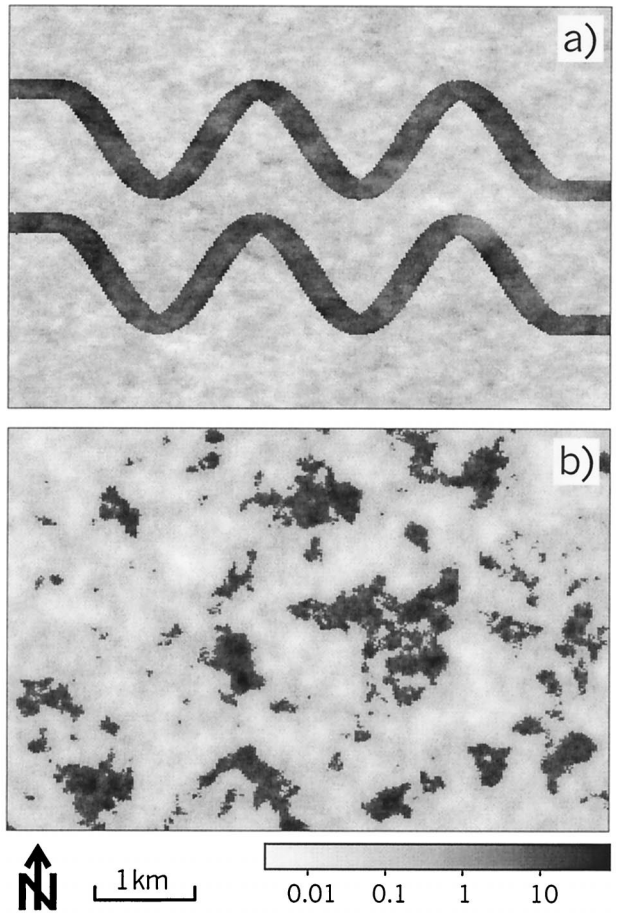

Figure 3. Hydraulic conductivities of two hypothetical aquifers with different degrees of connectivity. Values are in mm/s. (a) Connected conductivity pattern. (b) Random conductivity pattern generated using the turning bands method. Note that both patterns have the same probability density function (pdf) and variogram.

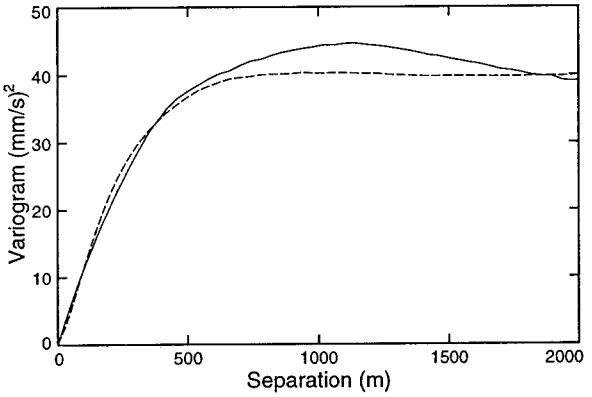

Figure 4. Omnidirectional variograms for the aquifer conductivity patterns shown in Figure 3.

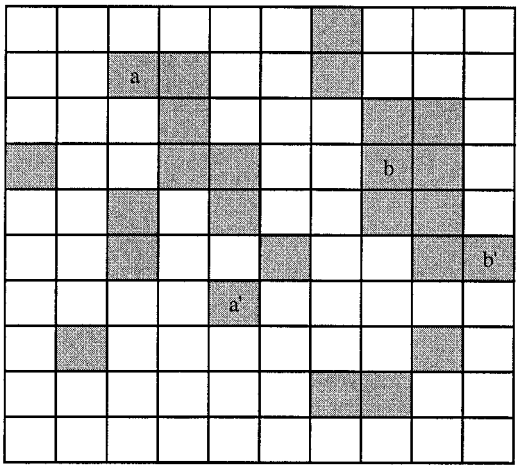

Figure 5. Definition of connectivity. The pairs of points (a, a') and (b, b') are connected, but a is not connected to b. The shaded cells represent $Z = 1$, and the white cells represent $Z = 0$.

methods used for each of these are given below. Omnidirectional connectivity considers all directions. When calculating omnidirectional connectivity, all pairs x and x' (where x has high moisture (or hydraulic conductivity)) are considered, and the path can progress from pixel to pixel along either the cardinal or the diagonal direction. Thus each pixel has eight neighbors (unless it is located on an edge). Topographically defined directional connectivity considers a subset of pairs x and x', for which x' is either up or down gradient of x. In this case the path was constrained so that it could only progress downslope (starting from x) via the two neighboring steepest descent pixels or upslope (starting from x) via any pixels which flowed through x (as determined by the two steepest descent directions). The gradients were defined using the digital elevation model for the Tarrawarra catchment [*Western and Grayson*, 1998] for the soil moisture case and the mean (effectively regional) head gradient for the groundwater case.

In this paper the connectivity functions were calculated using the following general steps. Pseudocode illustrating the implementation of the algorithms used to perform each of these steps is included in the electronic supplement.[1]

1. Step one is threshold the data into NO_DATA, LOW, and HIGH on the basis of the desired percentile value (50%, 75%, and 90% were used here)

2. Step two is label each continuous cluster with a unique label. We used a recursive algorithm to search by stepping from neighbor to neighbor in each cluster, labeling pixels as it goes. This process involves looping through all the pixels in the map, and whenever an unlabeled HIGH pixel is encountered, it is labeled with a unique label. Then a recursive search algorithm is used to check for any neighbors that are also HIGH (and thus connected). These neighbors are labeled with the same label as the original pixel, and the recursive algorithm is called again to search the next set of neighboring pixels. Note that the (potentially) global nature of connected regions requires that the entire indicator map be accessible at one time if this approach is used. Other approaches, including the Hoshen-Kopelman cluster assignment algorithm [*Gould and Tobochnik*, 1988] and an algorithm for mapping three-dimensional connectivity [*Deutsch*, 1998], can use row-by-row processing of the map.

3. Step three is calculate the connectivity function. The approach to this step depends on whether omnidirectional or topographic connectivity is calculated. (1) The first approach is omnidirectional. This involves looping through all pixels $[r, c]$ in the map. For those above the threshold a subloop is performed, which loops through all pixels $[rr, cc]$, in the map and results in pairs $([r, c], [rr, cc])$. For each pair their separation is determined, they are assigned to a separation bin, and the number of pairs in that bin is incremented. The pixels are connected if they have the same cluster label, in which case the number of connected pairs in that bin is also incremented. Once both these loops have been completed, the connectivity for each bin is calculated as the number of connected pairs divided by the number of pairs and the mean separation is also calculated. (2) The second approach is topographic. This involves looping through all pixels $[r, c]$. For those above the threshold, the pixels that contribute flow to $[r, c]$ and those that $[r, c]$ contributes to are mapped using a pair of recursive routines. The flow paths are determined on the basis of the two steepest descent directions. An alternative would be to prepare two maps of pointers to downslope cells and to search these recursively, which improves the computational efficiency but, unlike the algorithms used, does not handle the problem of identical slopes automatically. After the flow paths are mapped, a subloop is executed as for the omnidirectional connectivity functions described above. If a pixel $[rr, cc]$ is on a flow path to or from pixel $[r, c]$, then the separation is calculated, the pair is assigned to a separation bin, and the number of pairs in the bin is incremented. If both pixels in the pair have the same cluster label, they are connected, and the number of connected pairs in that bin is also incremented. Once both these loops have been completed, the connectivity for each bin is calculated as the number of connected pairs divided by the number of pairs, and the mean separation is also calculated.

3.2. Results

Figure 6a shows omnidirectional connectivity functions calculated for the 75th percentile indicator values from the 13 soil

[1]Supporting calculations are available via Web browser or via Anonymous FTP from ftp://kosmos.agu.org, directory "apend" (Username = "anonymous", Password = "guest"); subdirectories in the ftp site are arranged by paper number. Information on searching and submitting electronic supplements is found at http://www.agu.org/pubs/esupp_about.html.

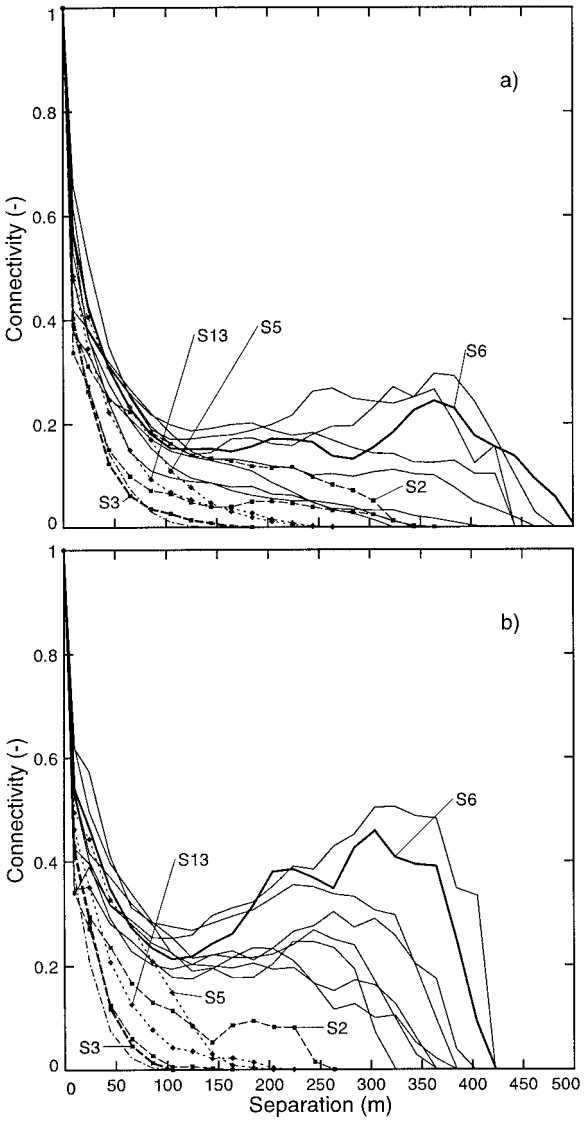

Figure 6. Connectivity functions $\tau(h)$ calculated for the 75th percentile indicator data from the Tarrawarra soil moisture patterns. (a) Omnidirectional connectivity and (b) directional (downslope) connectivity. The solid curves are for connected (wet) cases, the dashed curves with squares are for random (dry) cases, and the dotted curves with diamonds are for transition cases. The connectivity function for a random pattern generated using the turning bands method is also shown (dash-dotted curve without markers). Cases S3 and S6 are emphasized with heavier lines.

moisture patterns from Tarrawarra. The curves for the three patterns in Figure 1 are identified separately, and curves from dry periods (dashed curves with squares), wet periods (solid curves) and transition periods (dotted curves with diamonds) are indicated. The soil moisture patterns from wet periods clearly show connected bands in the drainage lines, while the dry patterns do not have connected bands in the drainage lines [*Western et al*., 1998b] (Figure 1). One would therefore assume that a significant amount of connectivity is present in the wet patterns, while very little connectivity is present in the dry patterns. Transition periods are when the pattern is changing from dry to wet or from wet to dry and the connectivity is developing or disappearing. Figure 6 indicates that there is a variety of shapes for the connectivity functions for different patterns. All patterns show an initial rapid decrease in connectivity to a value between 0.33 and 0.65 at a separation of 10 m (1 pixel). The connectivity then decreases more slowly. For some patterns the connectivity continues to decrease to zero at separations of 150–250 m (e.g., February 23, 1996, S3, which was a dry period). Some other patterns have connectivity functions that decrease at a moderate rate to zero at separations of ~350 m (e.g., April 13, 1996, S5, which was a transition period). The remaining patterns have high connectivity ($\tau(h) \approx 0.2$) for separations up to 400–500 m, which is large compared to the overall catchment extent, and then the connectivity decreases rapidly to zero (e.g., April 22, 1996, S6, which was a wet period). The difference in behavior is due to there being one or two large connected patches combined with a few small connected patches for the connected (wet) cases (e.g., S6), while there are only small connected patches for the disconnected (dry) cases (e.g., S3). Once the separation approaches the size of the largest patch, the connectivity rapidly approaches zero. Similar results were obtained for the 90th percentiles, although the values of connectivity were generally lower as a consequence of the higher percentile. At the 50th percentile the wet and dry patterns were less distinct. This is because the 50th percentile indicator patterns reflect low and high soil moisture values to the same extent, and hence the connectivity function reflects the connectivity of both dry and wet patches. Dry patches are not significantly connected, so the presence of connectivity does not appear as distinctly at the 50th percentile.

In general, the connectivity functions distinguish between the wet and dry cases quite well. The wet cases tend to exhibit high-connectivity functions, even at large scales, while the dry cases tend to have connectivity functions that rapidly approach zero. However, there is still not a perfect distinction between patterns where the flow paths are connected and disconnected. For example, S2 (February 14, 1996) shows significant connectivity up to a separation of 400 m, yet the pattern does not have a connected wet band in the drainage line [see *Western et al*., 1998b]. In this case the high connectivity at larger scales is due to connected bands of relatively high moisture along the contour rather than bands of moisture in the drainage lines. We would not expect the connectivity in S2 to be significant from a surface runoff perspective because the connectivity is not cooriented with the surface flow paths.

To improve the discrimination between patterns with and without connected high soil moisture bands in the drainage lines, we looked at directional connectivity functions. The direction was chosen to coincide with the direction of surface flow paths, as indicated by the surface topography. Figure 6b shows the directional connectivity functions for each survey. Now the connectivity functions for the three dry patterns are very similar to the connectivity functions for a random field, which is also shown on Figure 6b (dash-dotted curve without markers). The eight wet patterns show high connectivity. There are two intermediate directional connectivity functions. The first is for S5 (April 13, 1996), which represents the seasonal wetting transition during which connected wet bands in the drainage lines developed. The second is for S13 (November 29, 1996), which represents the seasonal drying transition during which connectivity disappears.

Table 1 includes the integral connectivity scales I_τ calculated from the directional connectivity functions for all three percentiles. The important result is that the connectivity scales for

the wet patterns are almost 10 times as large as the connectivity scales for the dry patterns (75th and 90th percentiles). Compared to the 75th percentile, the 50th percentile has longer integral connectivity scales because the connected regions tend to be larger due to the lower threshold. The 90th percentile has shorter integral connectivity scales for analogous reasons. In general, similar results were obtained for the seasonal pattern of changes in integral connectivity scales for all three percentiles, particularly for the 75th and 90th percentiles. There are some subtle differences in the temporal pattern of changes in the integral connectivity scale at the 50th percentile. These are due to increased integral connectivity scales associated with relatively wet south facing slopes during periods where there is a strong aspect influence on soil moisture. The influence of aspect on soil moisture at Tarrawarra is analyzed in greater detail by *Western et al*. [1999].

We also calculated connectivity functions for the two synthetic aquifers, one random and one with connected high-conductivity flow paths (Figure 7). As is the case for the soil moisture patterns, the omnidirectional connectivity functions for the connected and the random cases are very different. For the random aquifer the connectivity functions (dashed curves) drop rapidly to zero at separations around 2000 m, while for the connected aquifer, which exhibits paleochannels, the omnidirectional connectivity function (solid line) decreases relatively slowly for separations between 600 and 9000 m. These results are qualitatively very similar to those of the soil moisture patterns in terms of capturing the connectivity. Clearly, the hypothetical aquifers represent ideal random and connected patterns, and hence the connectivity functions are very different. It is interesting that at very short separations (shorter than 500 m) the connectivity functions in Figure 7 are similar. This is because 500 m is about the width of the paleochannels in Figure 3a, and at scales smaller than the width the pattern is essentially random and hence similar to the random pattern in Figure 3b. We have also calculated directional connectivity functions for both the west-east and north-south directions for the paleochannel case (Figure 7b). Here the regional (average) head gradient across the aquifer was used to define the directions in a similar manner to the use of topography in the soil moisture case. In real groundwater problems the regional head gradient is usually known from well information in groundwater studies. In the east-west direction, extensive connectivity is indicated by the connectivity function as would be expected given the pattern of hydraulic conductivity. In the north-south direction the connectivity is similar for both the random and connected cases. The directional integral connectivity scales (Table 2) for the paleochannel case correlate well with the extent of the paleochannels in each direction.

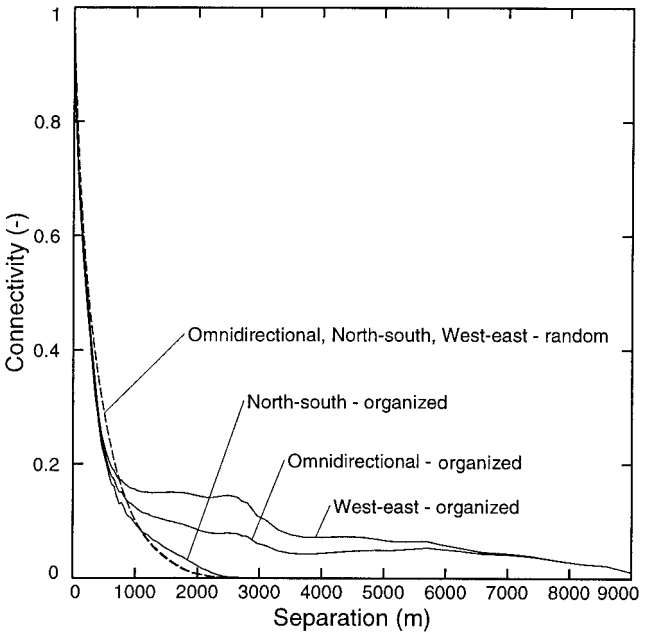

Figure 7. Omnidirectional and directional connectivity functions $\tau(h)$ calculated for the 75th percentile indicator data from the aquifer conductivity patterns shown in Figure 3. The solid curves are for the connected case, and the dashed curves are for the random case. The directionality of the functions is shown in the labels.

Table 2. Integral Connectivity Scales for the Synthetic Aquifers

Pattern	Direction[a]	Threshold 50%	Threshold 75%	Threshold 90%
Organized	omni	3272	746	247
Organized	north	2268	366	230
Organized	east	3403	946	266
Random	omni	1113	397	215
Random	north	1115	398	216
Random	east	1091	400	213

[a]Here omni is omnidirectional. The mean hydraulic conductivity is 0.233 mm/s, its variance is 0.434 $(mm/s)^2$, and the 50th, 75th, and 90th percentiles are 0.122, 0.240, and 9.08 mm/s, respectively. Note that the integral connectivity scales I_τ are larger for the organized pattern than for the random pattern when taken in east-west direction (east) and all directions (omni), particularly for the 75% threshold where the paleochannels are most apparent.

The above results indicate that the omnidirectional connectivity functions [*Allard*, 1994] discriminate between connected and disconnected flow paths quite well. By taking into account topographic information about expected surface flow paths in the soil moisture case, it is possible to further improve the discrimination between connected and disconnected patterns of hydrologic relevance. Similarly, by taking the regional head gradients into account, directional connectivity can also provide additional information in the groundwater case, which is also hydrologically more meaningful.

4. Hydrologic Simulations

4.1. Surface Runoff

In this section we use the Thales hydrologic model [*Grayson et al*., 1995] to explore how differences in connectivity might affect the surface runoff dynamics at Tarrawarra. The model implementation is similar to that presented by *Grayson et al*. [1995], with the numerical scheme modified to be an upwind implicit scheme. The surface runoff response at Tarrawarra is dominated by saturation excess overland flow [*Western and Grayson*, 1998]. Therefore we used Thales to model saturation excess runoff, kinematic overland flow, kinematic subsurface flow, and runon infiltration in the catchment. Large infiltration capacities were assumed, which means that all rainfall and overland flow entering a model element infiltrates unless the element is saturated. All soil parameters and surface flow resistance parameters were assumed to be spatially uniform. The

Table 3. Summary of the Rainfall Cases for the Rainfall-Runoff Simulations at Tarrawarra[a]

Case	Peak 6 min. Intensity, mm/h	Total Rainfall Depth, mm
1	43 (<1)	13.2 (<1)
2	65 (2)	19.8 (2)
3	86 (5)	26.4 (5)
4	129 (30)	39.6 (40)

[a]The average recurrence interval (years) for each rain case is given in parentheses. The same temporal pattern is used for each case (Figure 8a).

ability of a daily version of this model to predict spatial soil moisture patterns and runoff from the catchment was extensively tested by *Western and Grayson* [2000]. The aim of these simulations is to demonstrate that the connectivity function is related to simulated hydrologic behavior and therefore provides a useful statistical summary of pattern characteristics. If this can be established, it suggests that the connectivity statistics could provide a useful basis for developing a parameterization of subgrid variability in large-scale models or could be used to simulate realistic patterns (i.e., patterns conditioned on the connectivity function) of initial conditions for event-based catchment models. Patterns of initial conditions are always required to run these models, but they are generally not measured.

Two sets of simulations were performed using the Tarrawarra catchment. The simulations differ in the way the initial conditions were set. Setting initial conditions is a critical step in the majority of detailed runoff event simulations as these models are not generally run over extended periods. Given that it is known that the models are sensitive to the patterns used, it is important that the patterns used are appropriate. The aim here is to explore the relative importance of different parameters that can be used to characterize the spatial structure of the patterns statistically and thereby understand what the most important features of the patterns are. Identical probability density functions (similar to survey 1) were used for the simulations in order to control for the effects of soil moisture mean and variance. Thus differences in the simulations are related to differences in the spatial arrangement of moisture only.

The first set of simulations was based on the 13 measured soil moisture patterns. These were transformed so that each moisture pattern had the same soil moisture probability density function (pdf) as survey 1. The transformation was applied to the soil moisture value for a pixel without shifting the pixel's location. This implies that the spatial arrangement of the measurements was unchanged, which means that the indicator patterns and the connectivity functions were also unchanged. Thus the only difference between the 13 initial condition patterns is in the spatial arrangement of the soil moisture. Three different rainfall series were applied to each initial soil moisture pattern. These are typical of rainfall patterns observed at Tarrawarra, and each rainfall series has the same temporal pattern. They differ from each other in intensity. The rainfall cases are summarized in Table 3. The runoff response is summarized in terms of the total and peak discharge for each case.

Figure 8 shows hydrographs for random (February 23, 1996, S3, dashed curves) and connected (April 22, 1996, S6, solid curves) initial moisture patterns for each of the three rainfall cases. Figure 8a shows the 6 min rainfall intensities used to simulate the hydrographs in Figure 8b. For Figure 8c the rainfall intensity was increased to 150% of that in Figure 8a; for Figure 8d, it was increased to 200% of that in Figure 8a. There is a clear difference between the random and connected cases.

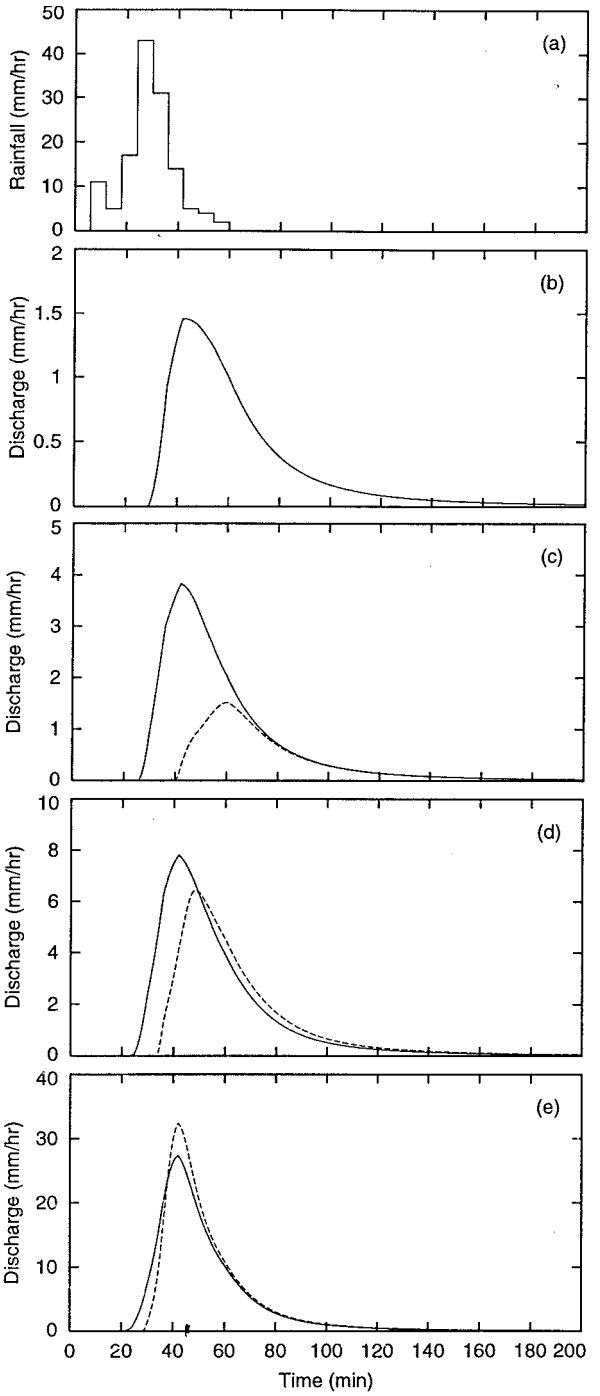

Figure 8. Simulated runoff hydrographs for the Tarrawarra catchment for three different assumed storms. Connected (April 22, 1996) and random (February 23, 1996) initial soil moisture patterns are used in the simulations. Note that the pdf of both initial moisture patterns has been transformed so that they are identical. The 6 min hyetograph in Figure 8a was used to simulate the hydrographs in Figure 8b, and it was multiplied by 1.5, 2.0, and 3.0 for the simulations in Figures 8c–8e, respectively.

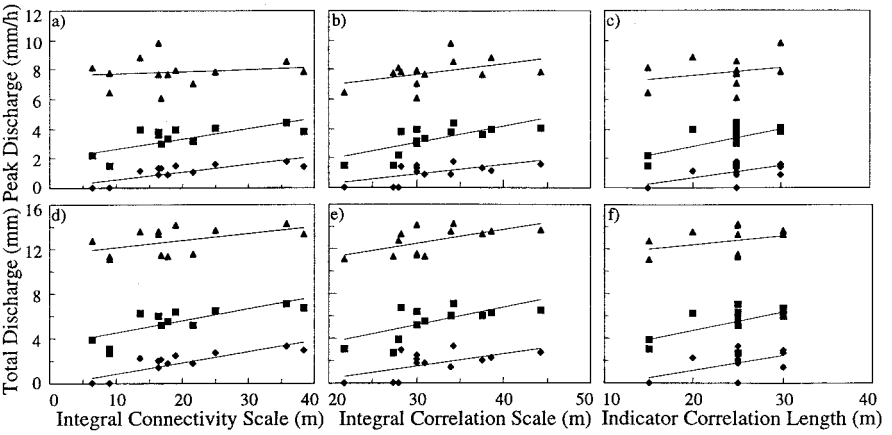

Figure 9. The variation in simulated peak (Figure 9a) and total discharge (Figure 9d) with directional connectivity scale I_τ for different assumed storms. The 90th percentile integral connectivity has been used. Diamonds indicate rain case 1, squares indicate rain case 2, and triangles indicate rain case 3. Figures 9b and 9e show similar relationships with integral correlations scale. Figures 9c and 9f show similar relationships with the 90th percentile indicator variogram correlation length.

The connected case produces runoff significantly earlier than the random case because the drainage line is already close to saturation. It also produces higher total and peak runoff rates for the smaller rainfall bursts. Figure 8e shows a very intense rainfall burst of 39.6 mm or 300% of case 1, which is equivalent to a 30–40 year rainstorm for the Tarrawarra climate. For this very intense rainfall the random case produces higher total and peak runoff rates because full connectivity occurs earlier than with the connected case.

Figures 9a–9c provide summaries of peak discharge as a function of integral connectivity and integral correlation scales and the indicator variogram correlation length, respectively, for each of the three rainfall cases to illustrate the type of information provided by the two statistical measures. We have used the omidirectional connectivity at the 90th percentile for Figure 9a and the 90th percentile indicator variogram for Figure 9c. Figures 9d–9f provide the same summary for total runoff. The integral connectivity scale was calculated using the omnidirectional connectivity functions (Figure 6b) and a discrete version of (2). The integral correlation scale was calculated from the fitted variograms [*Western et al*., 1998a]. The indicator variogram correlation length was estimated by fitting an exponential variogram with nugget [*Western et al*., 1998b]. The larger the integral connectivity scale, the more dominant the wet bands in the drainage line are. That is, random patterns plot on the left side of Figures 9a and 9d, while connected patterns plot on the right side. Wet cases also have a weak tendency for high integral correlation scales, although there is not a strong relationship between the correlation scale and the presence of connectivity.

Figure 9 illustrates that the basic trends evident in Figure 8 hold when a larger sample of initial soil moisture patterns is considered. The changes in peak and total discharge with connectivity scale are quite significant. For the low rainfall case (Figures 9a and 9c, diamonds) the peak and total discharge increase from close to zero to 2 mm/h and 3.5 mm, respectively, as the connectivity scale increases. In the intermediate rainfall case (squares) the peak discharge increases by ~190% from 2.4 to 4.6 mm/h, while the total discharge increases by ~190% from 4.0 to 7.5 mm. For the highest rainfall case (triangles) the peak discharge remains almost constant at ~8 mm/h as the connectivity increases, and the total discharge increases by 16% from 11.9 to 13.8 mm as the connectivity increases. There is also some scatter around the general trends. Similar patterns are observed in the relationships between runoff and both the integral correlation scale and the indicator variogram correlation length. Table 4 demonstrates that runoff is more closely related to connectivity for all the events, provided an appropriate percentile threshold is chosen. The appropriate percentile threshold reduces as the amount of rainfall increases because a greater proportion of the catchment is saturating and contributing to the runoff. There is also a tendency for smaller events (typical of most of those observed at Tarrawarra) to be more highly correlated with both connectivity and correlation scales than for extreme events (Table 4). There is no clear evidence that runoff behavior is more strongly related to either one of the omnidirectional or topographic connectivity functions used here.

In the second set of simulations, patterns of initial soil moisture with varying connectivity but similar variograms were constructed. This was achieved by generating a random pattern with a similar variogram to survey 1 [*Western et al*., 1998a] using the turning bands method. Weighted combinations of this random pattern and the measured pattern from survey 1 were calculated. Then the pdf of the combined pattern was transformed to be the same as survey 1. Six different weightings were used: 100% random, 80% random and 20% survey 1, 60% random and 40% survey 1, 40% random and 60% survey 1, 20% random and 80% survey 1, and 100% survey 1. Sixteen realizations of each of these combinations were calculated. Figure 10 shows the variograms and connectivity functions (averaged over the 16 realizations) for the six different weightings. Simulations were run on the three rainfall cases used in Figure 8, and peak and total discharges (averaged over the 16 realizations) were calculated for each of the six weightings. Average topographic integral connectivity scales at the 50th, 75th, and 90th percentiles were also calculated for the six weightings.

Figure 11 shows that for the small and medium rainfall events both average peak and average total discharge increase as the degree of connectivity increases. Each point represents responses averaged over 16 realizations. For the largest rainfall

Table 4. Coefficient of Determination for Relationships Between Runoff Behavior and Integral Correlation Scale, the Indicator Variogram Correlation Length (From Fitted Exponential Variograms), and the Integral Connectivity Scale for the Simulations Using the 13 Observed Soil Moisture Patterns From Tarrawarra[a]

	Peak Discharge, mm/h			Total Discharge, mm		
	Rain × 1	Rain × 1.5	Rain × 2	Rain × 1	Rain × 1.5	Rain × 2
Integral correlation scale	0.38	0.50	0.20	0.35	0.43	0.36
Indicator correlation length						
50%	0.36	0.30	0.02	0.32	0.32	0.01
75%	0.40	0.35	0.00	0.40	0.33	0.02
90%	0.40	0.36	0.08	0.39	0.35	0.11
Integral connectivity scales						
50% omni	0.25	0.46	0.29	0.31	0.45	0.26
50% topo	0.52	0.73	0.23	0.55	0.71	0.36
75% omni	0.48	0.31	0.01	0.49	0.36	0.22
90% omni	0.61	0.49	0.02	0.71	0.58	0.24
75% topo	0.48	0.31	0.02	0.50	0.35	0.04
90% topo	0.56	0.42	0.01	0.66	0.52	0.26

[a]Note that the soil moisture pdf was normalized to survey 1 for each simulation. Here omni is omnidirectional, and topo is topographic.

event the average total discharge increases, but the average peak discharge decreases slightly as connectivity increases. Comparing Figures 9a with 11a and 9c with 11b indicates that the changes in runoff response with connectivity scale are very similar for the two different sets of simulations. In all but the case of peak runoff for the largest event (which has only a small variation in the runoff response) the connectivity scale explains >90% of the variation in runoff response (Table 5). It is important to remember that the variograms are held constant (i.e., integral correlation scale is the same) while the connectivity is varied in this set of simulations.

4.2. Groundwater Solute Transport

In this section we use a finite element groundwater model [*Blöschl and Blaschke*, 1992] to explore how differences in connectivity might affect the transport dynamics of an aquifer. The model is two-dimensional in the horizontal, while the vertical dimension is lumped. Two sets of simulations were

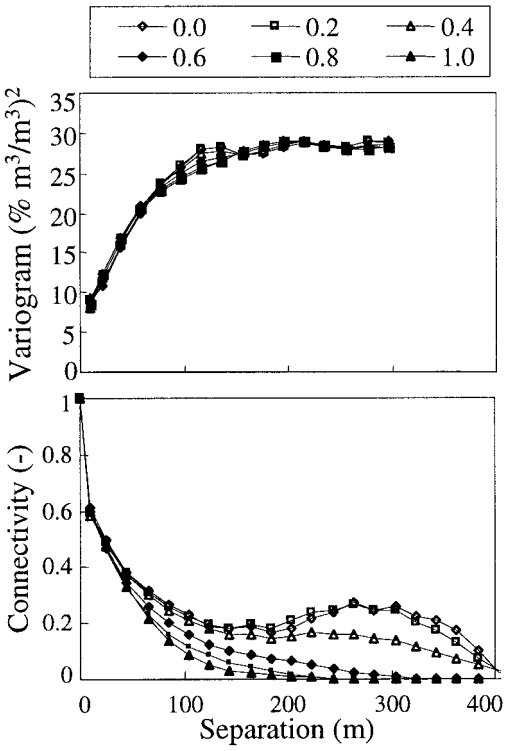

Figure 10. Average variograms and topographic connectivity functions (75% threshold) for the initial soil moisture patterns generated by weighting the observed pattern from survey 1 with a random pattern that was generated using the fitted variogram for survey 1.

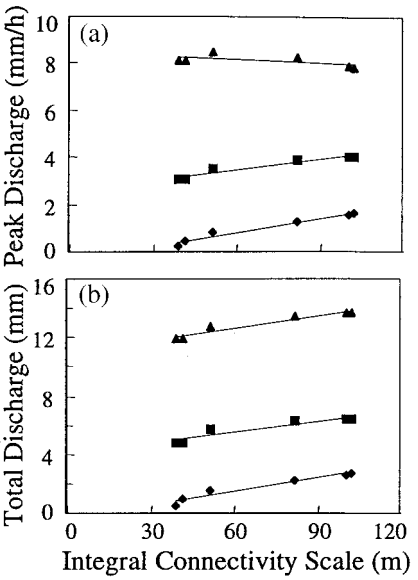

Figure 11. The variation in simulated (a) peak and (b) total discharge with directional connectivity scale I_τ for different assumed storms. The initial soil moisture patterns were generated by weighting the observed pattern from survey 1 with a random pattern that was generated using the fitted variogram for survey 1. Each symbol represents the average of 16 realizations with a constant weighting of observed and random pattern. Diamonds, squares, and triangles indicate rain cases 1, 2, and 3, respectively.

Table 5. Coefficient of Determination for Relationships Between Average (Over 16 Realizations) Runoff Behavior and Integral Connectivity Scales for the Simulations Using the Patterns With Varying Organization (Mix of Survey 1 and Random)[a]

Integral connectivity scales	Peak Discharge, mm/h			Total Discharge, mm		
	Rain × 1	Rain × 1.5	Rain × 2	Rain × 1	Rain × 1.5	Rain × 2
50% omni	0.99	0.98	0.16	0.99	0.97	0.98
50% topo	0.93	0.94	0.16	0.94	0.93	0.95
75% omni	0.90	0.87	0.43	0.87	0.83	0.86
75% topo	0.96	0.94	0.32	0.95	0.91	0.93
90% omni	0.12	0.07	0.87	0.08	0.04	0.06
90% topo	0.65	0.58	0.74	0.59	0.51	0.55

[a]Note that the soil moisture pdf was normalized to survey 1 for each simulation.

conducted for the aquifers in Figure 3. The first had flow from west to east driven by prescribed heads at these boundaries, with the northern and southern boundaries assumed to be impervious. The second had flow from north to south and was driven by prescribed heads with impervious eastern and western boundaries. The mean hydraulic gradient of the aquifer was the same for both flow directions and was equal to 30/9000 = 20/6000. The porosity was 0.1. The small-scale (within element) dispersivity was set to zero, which means that dispersion only occurs at a scale that is resolved by the groundwater model. Breakthrough curves were calculated for each aquifer based on a step input of concentration at the upstream boundary. A sharp transition between high and low conductivities at the interface between paleochannels and the ambient medium may cause problems in numerical transport algorithms. To avoid potential problems with conventional particle tracking (random walk) procedures [see, e.g., *Cordes and Kinzelbach*, 1992; *LaBolle et al*., 1996], an alternative approach for estimating the breakthrough curve was adopted [*Blöschl*, 1996]. Specifically, the flow system was solved twice. The first simulation provided the flow velocities in each element. The second simulation was a conjugate simulation that builds on the symmetry between the potential and the stream functions. The conjugate case uses swapped contour lines and stream lines and uses conjugate (swapped) boundary conditions as well as the inverse of conductivities. The conjugate case gives contour lines of heads, which can be interpreted as stream lines of the original case. The algorithm then integrates numerically the values of the velocities of the first (original) case along the flow directions (i.e., stream lines) of the second (conjugate) case, which yields arrival times and, as their cumulative distribution function, the break through curve. It is clear that this approach is very accurate and avoids the problems one encounters with other methods when high-conductivity contrasts (discontinuities) are present in the aquifer.

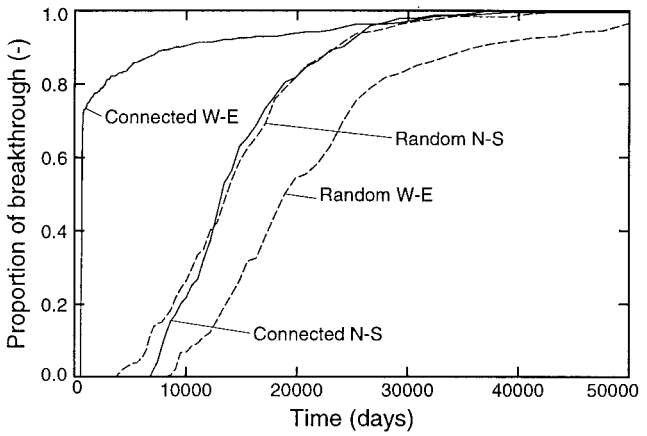

Figure 12. Breakthrough curves based on a step increase of concentration at the western boundary with west-east flow and at the northern boundary with north-south flow. The breakthrough curves were computed using a finite element model for the two aquifer conductivity patterns shown in Figure 3.

The breakthrough curves so estimated are shown in Figures 12a and 12b for both north-south and west-east flow directions. For west-east flow in the connected aquifer with the high conductivity paleochannels the median response (50% of concentration) occurs after 670 days (1.8 years), while in the random case the median response occurs only after 18,900 days (51.8 years). The large difference is due to the rapid flow through the high-conductivity flow paths in the connected case. Judged on the basis of standard geostatistical measures (e.g., the variogram, the integral correlation scale, and the probability density function), these aquifers are statistically similar; however, their connectivity functions are very different. From a groundwater dynamics perspective the connectivity functions clearly characterize an important feature of the spatial pattern of conductivities. For north-south flow the break through curves are very similar with the median response occurring at ~13,500 days (37 years). The connectivity in the north-south direction is also similar for both cases.

Qualitatively, the groundwater results are similar to the soil moisture cases, and the response dynamics are closely related to the integral connectivity scales as calculated from Figure 7. For the west-east direction in the connected aquifer, $I_\tau = 946$ m, which translates into a fast median response (1.8 years), while for the random aquifer, $I_\tau = 400$ m, which translates into a much slower median response (51.8 years). For north-south flow in both aquifers the integral connectivity scale and the breakthrough behavior are similar.

5. Discussion and Conclusions

Our results indicate that unlike more standard geostatistical approaches, the connectivity function approach [*Allard*, 1994; *Allard and Group*, 1993] is able to discriminate between spatial patterns that exhibit very different connectivity characteristics. In the case of the soil moisture patterns, there are clear differences between wet and dry patterns in terms of the connectivity along the topographically determined surface flow paths that are detected by the connectivity functions. Indicator variograms were unable to distinguish between the wet and dry

patterns [*Western et al*., 1998b]. Rainfall-runoff simulations showed that the runoff responses varied as the connectivity of the moisture patterns varied when the pattern's variogram was held constant. Even when the variogram changes between patterns, the runoff response was more closely related to the integral connectivity scale than to the integral correlation scale. The connectivity approach also distinguished between the two synthetic aquifers, even though the patterns are essentially identical in terms of their pdf, variograms, and anisotropy. Our simulations also show that the different patterns exhibit hydrologically different behavior. Therefore we can conclude that the connectivity function is characterizing features of the patterns that are hydrologically significant and that the approach is superior to the more standard geostatistical approaches in terms of capturing connectivity.

It is possible to relate the differences in connectivity to the differences in hydrologic behavior by considering the processes controlling the system's behavior. In the groundwater case it is clear that the rapid transport is due to high flow velocities through the well-connected high-conductivity zones. The difference in median breakthrough time between the connected and disconnected cases is more than an order of magnitude (1.8 and 51.8 years, respectively, for west-east flow), which is very significant from a practical perspective. It is important to realize that while the aquifers used in the example are artificial, they are related to real groundwater systems in that the connected case provides an idealization of paleochannels which are important features of many alluvial aquifers.

A somewhat related analysis of groundwater transport has been performed by *Scheibe* [1993], who examined a number of hypothetical aquifers exhibiting realistic sedimentary structures. *Scheibe* [1993] characterized the conductivity patterns of these aquifers by a number of statistical measures, including connectivity measures, and related these to the transport dynamics of these aquifers. While *Scheibe*'s [1993] results are qualitative in nature, he did find that the connectivity measures were related to the early breakthrough times and to the mean velocity with highly connected patterns being associated with earlier breakthrough. This is consistent with the results in this paper. *Gómez-Hernández and Wen* [1997] also found significant differences in transport behavior for patterns with qualitatively different connectivity features; however, they did not quantify the degree of connectivity.

In the case of soil moisture the high-connectivity patterns produce more runoff, in terms of both peak flows and total discharge, for small rainfall totals (Figures 8, 9, and 11), while in some cases (Figures 8e and 11) the low-connectivity patterns can produce higher peak discharges for large rainfall totals. This behavior can be explained as follows. Both the random and connected cases start with statistically similar moisture contents. This means that both start with the same proportion of the catchment saturated (or with any specified saturation deficit). When the rain begins, the connected case produces runoff at the catchment outlet early because most of the wet areas are in the gully and there is little runon infiltration downstream of the saturated source areas. In the random case the saturated source areas are mainly on the hillslopes, and there is a much greater opportunity for runon infiltration before the overland flow leaves the catchment; hence the total runoff is less. In most cases the saturated area connected to the outlet is larger at the time of the peak rainfall rate for the connected cases, and this leads to larger peak runoff. However, after a large amount of rainfall, the opposite can be true. As rainfall continues, more of the saturated source area runoff is contributing to an increase in the total saturated area in the random case, whereas more is leaving the catchment as overland flow in the connected case. Therefore, compared to the connected case, the total saturated area can grow more quickly in the random case. Once this increasing saturated area connects to the catchment outlet, the random case produces greater discharges. If the simulations are continued until the rainfall totals are sufficient to saturate the majority of the catchment, the behavior of the random and connected cases eventually converges.

While the differences in runoff behavior for soil moisture patterns with different connectivity are not as dramatic as for the groundwater case, they are still significant (190% for both peak runoff and total runoff in moderate events), and the underlying trend is clearly evident against the random scatter. The scatter appears to be related to the proximity of wet patches to the drainage lines, which varies randomly (at least in part) between patterns. This variation influences the runoff behavior at the catchment outlet by affecting the connection of saturated areas to the catchment outlet. Some of this randomness is due to measurement error, and some is likely to be due to small-scale variability, which is not averaged out by the point measurements. It is also likely that varying antecedent forcing combined with the catchment dynamics leads to complex variations in the details of the observed patterns.

We expect that this randomness will be scale dependent. At larger scales some of the randomness might be averaged out owing to more representative integration within the channel network. However, any scale effects will also depend on what happens to the spatial variability in moisture at larger scales. Other sources of variability will also arise at larger scales, including differently shaped subcatchments and variability in geology, soils, vegetation, and land use.

Somewhat similar results have been obtained for catchment runoff by *Grayson et al*. [1995]. They used antecedent soil moisture patterns that were identical in terms of their pdf and variograms in simulations of runoff from a hypothetical catchment based on the Coweeta topography and found that simulated runoff varied substantially between connected and disconnected antecedent patterns. Rainfall characteristics influenced the runoff in their simulations in a similar way to ours. This is related to the representation of similar processes in the study of *Grayson et al*. [1995] and in this paper. In both cases, saturation excess runoff and runon infiltration were the dominant mechanisms. In contrast, *Merz and Plate* [1997] examined the effect of connectivity of the patterns of initial soil moisture on simulated runoff for a catchment where Hortonian (infiltration excess) overland flow is the dominant mechanism. They found that for small events and for large events, there is only a minor effect of the spatial arrangement of soil moisture on simulated runoff, while there is a substantial effect for intermediate events. For small events, only the sealed parts of the catchment (i.e., mainly the roads) contribute to runoff. For large events the source areas are widely spread over the catchment, and one would therefore not assume the spatial arrangement of soil moisture to be important for runoff generation. However, for intermediate events where rainfall intensity is of the same order of magnitude as saturated hydraulic conductivity, there is a substantial effect on runoff of up to double the runoff peaks and 3 times the event runoff volumes in the connected case as compared to the disconnected case. While *Merz and Plate* [1997] found the rainfall intensity relative

to soil hydraulic conductivity to be important in controlling the effect of the connectivity on runoff, in this paper, event rainfall depth relative to saturation deficit is likely to be an important parameter as the saturation excess mechanism prevails. It is also important to note that this paper goes beyond the previous work mentioned above in using observed spatial soil moisture patterns (as opposed to assumed patterns) and in quantifying connectivity by the connectivity function and the integral connectivity scale (as opposed to qualitative descriptions of connectivity).

We believe that the effect of connectivity on hydrologic response demonstrated here for two examples (catchment runoff and groundwater transport) is also valid for a much wider range of hydrologic processes, ranging from small-scale macropore flow in soils to the large-scale response of river basins. The link between the soil moisture case and the groundwater case is fundamentally to do with the provision of efficient flow paths. In an aquifer a flow path is efficient if the flow resistance is low, and in the soil moisture case a flow path is efficient if the losses to runon infiltration are low. The actual shape of these flow paths is not important; it is the fact that they are connected. A long and winding road is better than no road at all. This provides an insight into the reason why traditional geostatistical approaches fail in this context. They fail because there is an underlying assumption that the relationship between points is determined by their Euclidian separation alone. The connectivity functions work because they account for connected paths of arbitrary shape.

The importance of an efficient flow path also provides a criterion for determining whether or not directionality is important when considering connectivity functions. Where flow paths are aligned with the connectivity, the connectivity plays an important role. This is illustrated in the groundwater example where west-east transport was greatly affected by the (west-east oriented) connectivity but the north-south transport was not. Use of directional connectivity functions allowed these two cases to be easily distinguished in a quantitative manner. In the case of soil moisture the surface flow paths are determined by the topography. The topographically determined flow paths do not necessarily coincide with connected high soil moisture bands in a pattern. For example, where the underlying geological formations are dipping into a hillslope, bands of different soil moisture may develop across the hillslope due to different soil characteristics. This means that directionality is likely to be more important, although the omnidirectional connectivity functions do still distinguish between the patterns quite well, whereas the variogram-based approaches do not. Thus it is likely that consideration of directionality will be important wherever the feature being considered does not control the flow path. This is the case in the soil moisture example where the soil moisture controls the runoff generation and the topography determines the flow path. Of course, there is a strong tendency for these two to interact to produce connectivity of soil moisture that coincides with the topographically determined flow paths.

We have demonstrated that connectivity statistics can capture hydrologically significant features of spatial patterns and have discussed the process considerations that support the link between connectivity and hydrologic behavior. An obvious question now is how one would use the connectivity statistics in practical hydrologic applications. We envisage four potential applications and associated issues: (1) estimation of connectivity statistics from data, (2) estimation of spatial patterns from point data (i.e., interpolation and stochastic simulation), (3) use of the integral connectivity scale as a bulk parameter to characterise hydrologically relevant spatial characteristics of patterns, and (4) scale dependence of the connectivity statistics.

5.1. Estimation of Connectivity Statistics From Data

Unlike traditional geostatistics where the variogram can be estimated from a number of point values in the domain, the estimation of the connectivity function requires that the pattern must be exhaustively known. This is because in the case of the variogram the spatial (Euclidean) distance between pairs of points (along with the point data values) determines the variogram, while in the case of the connectivity function it is also the spatial arrangement of the underlying pattern that determines the connectivity function. In most practical cases, including those that the soil moisture and groundwater examples in this paper stand for, an exhaustive spatial pattern will not be known. To obtain realistic values for the connectivity function in such cases, one possibility is to use "proxy" or "soft" data. For example, in groundwater hydrology the spatial arrangement of geologic formations as seen in outcrops or in underground mines [see *Williams*, 1988] is an important piece of information for obtaining an idea of the spatial structure of the subsurface. This type of soft information can be used to estimate, at least approximately, the connectivity function because the connectivity function builds on indicator values (either 0 or 1) similar to those used in indicator geostatistics [*Journel*, 1983] where soft information has been widely used in the past [e.g., see *Anderson*, 1997]. If soft data are not available, an alternative is to transpose values of the connectivity function or the integral connectivity scale from studies one would think exhibit similar behavior, in very much the same way as is done currently in many practical applications. For example, values of dispersivity and hydraulic soil properties are transposed from one study site to another.

5.2. Estimation of Spatial Patterns From Point Data (Interpolation and Stochastic Simulation)

Here, again, the fact that the connectivity approach depends on the spatial arrangement of the pattern between data points (unlike traditional geostatistics) is important. Because of this a simple extension of the more commonly used geostatistical techniques (such as kriging and sequential indicator simulation) to accommodate the connectivity function is probably not easily possible. However, a number of pattern generation techniques are more flexible, and it is straightforward to accommodate the connectivity function in them. For example, simulated annealing [*Srivastava*, 1994; *Deutsch and Cockerham*, 1994] is an iterative method of generating patterns that minimizes the difference between statistics of the pattern to be generated and the statistics of a training image. The choice of the control statistics is critically important in creating realistical looking patterns. If one uses, say, indicator variograms as control statistics, the simulated pattern will be similar to that generated by indicator based stochastic methods such as sequential indicator simulation [*Deutsch and Journel*, 1992]. One can now use the connectivity function (or the integral connectivity scale alone) as the control statistics. If one prescribes a connectivity function, there is no need for a training image. Simulated annealing will then generate patterns with realistic connectivity features. Simulated annealing can be used both for interpolating between point values if data are available (conditional simulation) and for generating spatial patterns

with realistic connectivity features if no data are available (unconditional simulation). It should be noted that while simulated annealing approaches are computationally very demanding, one can expect that they will become more widely used in the future with the current trend of decreasing computing costs.

5.3. Use of the Integral Connectivity Scale as a Bulk Parameter to Characterize Hydrologically Relevant Spatial Characteristics of Patterns

There are a number of disciplines that have a long history in using the integral correlation scale as a bulk descriptor of spatial (or temporal) variability. Examples include fluid dynamics [*Taylor*, 1921; *Prandtl*, 1925], where the concept of an integral correlation scale was first conceived, and there are numerous applications in various areas of hydrology [e.g., *Rodríguez-Iturbe*, 1986; *Dagan*, 1989; *Gelhar*, 1993]. Common to all of these approaches is that instead of the full spatial complexity, they use only one number (the integral correlation scale) as a key parameter. One can envisage, say, a stochastic groundwater theory that builds on the integral connectivity scale rather than on the integral correlation scale. In this example the integral connectivity scale will be dependent on the mean flow direction (as in the example in Figure 7), which perhaps makes the usage of the integral connectivity scale more difficult but certainly makes it more appealing from a physical perspective. Another potential application is the use of the integral connectivity scale as a bulk parameter to characterize subgrid variability in large-scale surface hydrological problems, such as the description of the land surface in atmospheric global circulation models and numerical weather prediction models. One would expect that at these very large scales the connectivity of hydrologic patterns will also be very important from a hydrologic perspective.

5.4. Scale Dependence of the Connectivity Statistics

In this paper we have used fixed pixel sizes (10×20 m in the soil moisture case and 23.4×23.4 m in the groundwater case) to estimate the connectivity function. It is quite obvious that the connectivity function will change as the pixel size changes. This is similar to standard geostatistics where the pixel size is termed block size or support, and their effect on the probability density function and the variogram can be estimated by regularization techniques. In fact, estimating the effect of pixel size (or support) has been one of the main motivations for the emergence of geostatistics [*Journel and Huijbregts*, 1978]. Regularization techniques have been used in various areas of hydrology, including precipitation [*Rodríguez-Iturbe and Mejía*, 1974; *Sivapalan and Blöschl*, 1998], surface hydrology [*Western and Blöschl*, 1999], and of course, groundwater hydrology [e.g., see *Wen and Gómez-Hernández*, 1996]. One can envisage similar regularization techniques for the connectivity function approach, which would provide a means of obtaining the connectivity function valid at a small pixel size from a connectivity function valid at a large pixel size and vice versa. This scale effect is related to the issue of near connectedness. For example, two large wet patches with a single dry pixel in between are not strictly connected, but they may have a similar impact on runoff response to the case where the single pixel is in fact wet and only one large connected region exists. Similarly, in the groundwater case, high-conductivity bands that are nearly connected may have a similar effect on groundwater dynamics as fully connected bands. Clearly, in both cases the apparent presence of near connectedness is scale dependent. As one aggregates a number of neighboring pixels to a large pixel, the single low-conductivity pixel (or the single dry pixel in the soil moisture case) will disappear, and the nearly connected bands will appear as one large band. However, as one keeps aggregating, the connected band will also disappear at some level of aggregation. The effect of near connectedness can therefore be dealt with in the context of the scale-dependent nature of the connectivity function. Another scale-related issue is that of stationarity. We have assumed that the connectivity function depends only on the scalar h, i.e. the spatial field is stationary. This is a common assumption in geostatistics and *Western et al.* [1998a, 1998b] have demonstrated that the soil moisture patterns are stationary. The synthetic aquifer patterns are also stationary. For application to nonstationary patterns some further development of the technique, such as incorporating a detrending step or using locally defined indicator statistics, would be required. This is also the case with standard geostatistical techniques [*Isaaks and Srivastava*, 1989]. The four issues discussed above will provide fertile ground for further research into the application of connectivity concepts in hydrology.

Acknowledgments. The Tarrawarra catchment is owned by the Cistercian Monks (Tarrawarra) who have provided free access to their land and willing cooperation throughout this project. Funding for the above work was provided by the Australian Research Council (project A39531077), the Cooperative Research Centre for Catchment Hydrology, the Oesterreichische Nationalbank, Vienna (project 5309), the Tewkesbury fund, a University of Melbourne Visiting Scholars Award, and the Department of Industry, Science and Tourism, International Science and Technology Programme. The second author wishes to thank Dieter Gutknecht for many enlightening discussions on spatial organization and patterns.

References

Allard, D., Simulating a geological lithofacies with respect to connectivity information using the truncated Gaussian model, in *Geostatistical Simulations: Proceedings of the Geostatistical Simulation Workshop, Fontainbleau, France, 27–28 May 1993*, edited by M. Armstrong and P. A. Dowd, pp. 197–211, Kluwer Acad., Norwell, Mass., 1994.

Allard, D., and H. Group, On the connectivity of two random set models: The truncated Gaussian and the Boolean, in *Geostatistics Tróia '92*, vol. 1, edited by A. Soares, pp. 467–478, Kluwer Acad., Norwell, Mass., 1993.

Anderson, M. P., Characterization of geological heterogeneity, in *Subsurface Flow and Transport*, edited by G. Dagan and S. P. Neuman, pp. 23–43, Cambridge Univ. Press, New York, 1997.

Bierkens, M. F. P., and H. Weerts, Block hydraulic conductivity of cross-bedded fluvial sediments, *Water Resour. Res.*, *30*, 2665–2678, 1994.

Blöschl, G., Scale and scaling in hydrology, *Wien. Mitt. Wasser Abwasser Gewässer*, *132*, 346 pp., 1996.

Blöschl, G., and A. P. Blaschke, HPP-GMS: A graphic user-interface for groundwater modelling, in *Hydraulic Engineering Software IV*, edited by W. R. Blain and E. Cabrera, pp. 523–537, *Comput. Mechn.*, Billerica, Mass., 1992.

Blöschl, G., and R. B. Grayson, Spatial observations and interpolation, in *Spatial Patterns in Catchment Hydrology—Observations and Modelling*, edited by R. B. Grayson and G. Blöschl, Cambridge Univ. Press, New York, in press, 2000.

Blöschl, G., and M. Sivapalan, Scale issues in hydrological modelling: A review, *Hydrol. Processes*, *9*, 251–290, 1995.

Blöschl, G., D. Gutknecht, R. B. Grayson, M. Sivapalan, and I. D. Moore, Organisation and randomness in catchments and the verification of distributed hydrologic models, *Eos Trans. AGU*, *74*(43), Fall Meet. Suppl., 317, 1993.

Bronstert, A., and A. Bárdossy, The role of spatial variability of soil

moisture for modelling surface runoff generation at the small catchment scale, *Hydrol. Earth Syst. Sci*., *3*, 505–516, 1999.
Clemo, T., and L. Smith, A hierarchical model for solute transport in fractured media, *Water Resour. Res*., *33*, 1763–1783, 1997.
Cordes, C., and W. Kinzelbach, Continuous groundwater velocity fields and path lines in linear, bilinear, and trilinear finite elements, *Water Resour. Res*., *28*, 2903–2911, 1992.
Dagan, G., *Flow and Transport in Porous Formations*, 465 pp., Springer-Verlag, New York, 1989.
Desbarats, A. J., and R. M. Srivastava, Geostatistical characterization of groundwater flow parameters in a simulated aquifer, *Water Resour. Res*., *27*, 687–698, 1991.
Deutsch, C. V., Fortran programs for calculating connectivity of three-dimensional numerical models and for ranking multiple realisations, *Comput. Geosci*., *24*, 69–76, 1998.
Deutsch, C., and P. Cockerham, Practical considerations in the application of simulated annealing to stochastic simulation, *Math. Geol*., *26*, 67–82, 1994.
Deutsch, C. V., and A. G. Journel, *GSLIB Geostatistical Software Library and User's Guide*, 340 pp., Oxford Univ. Press, New York, 1992.
Dunne, T., T. R. Moore, and C. H. Taylor, Recognition and prediction of runoff-producing zones in humid regions, *Hydrol. Sci. Bull*., *20*, 305–327, 1975.
Gavrilenko, P., and Y. Gueguen, Flow in fractured media: A modified renormalization method, *Water Resour. Res*., *34*, 177–191, 1998.
Gelhar, L. W., *Stochastic Subsurface Hydrology*, 390 pp., Prentice-Hall, Englewood Cliffs, N. J., 1993.
Gómez-Hernández, J. J., and X.-H. Wen, To be or not to be multi-Gaussian? A reflection on stochastic hydrogeology, *Adv. Water Resour*., *21*, 47–61, 1997.
Gould, H., and J. Tobochnik, *An Introduction to Computer Simulation Methods: Applications to Physical Systems*, part 2, 695 pp., Addison-Wesley-Longman, Reading, Mass., 1988.
Grayson, R. B., G. Blöschl, and I. D. Moore, Distributed parameter hydrologic modelling using vector elevation data: Thales and TAPES-C, in *Computer Models of Watershed Hydrology*, edited by V. P. Singh, pp. 669–695, Water Resources Publ., Highlands Ranch, Colo., 1995.
Grayson, R. B., A. W. Western, F. H. S. Chiew, and G. Blöschl, Preferred states in spatial soil moisture patterns: Local and nonlocal controls, *Water Resour. Res*., *33*, 2897–2908, 1997.
Grimmet, G., *Percolation*, 296 pp., Springer-Verlag, New York, 1989.
Gutknecht, D., Grundphänomene hydrologischer prozesse, *Zürcher Geogr. Schr*., *53*, 25–38, 1993.
Isaaks, E. H., and R. M. Srivastava, *An Introduction to Applied Geostatistics*, Oxford Univ. Press, New York, 1989.
Journel, A. G., Nonparametric estimation of spatial distributions, *Math. Geol*., *15*, 445–468, 1983.
Journel, A. G., and F. G. Alabert, Focussing on spatial connectivity of extreme-valued attributes: Stochastic indicator models of reservoir heterogeneities, paper presented at 63rd Annual Technical Conference and Exhibition, Soc. of Pet. Eng., Houston, Tex., Oct. 2–5, 1988.
Journel, A. G., and C. J. Huijbregts, *Mining Geostatistics*, 600 pp., Academic, San Diego, Calif., 1978.
Koltermann, C. E., and S. M. Gorelick, Heterogeneity in sedimentary deposits: A review of structure-imitating, process-imitating and descriptive approaches, *Water Resour. Res*., *32*, 2617–2658, 1996.
Kupfersberger, H., and G. Blöschl, Estimating aquifer transmissivities—On the value of auxiliary data, *J. Hydrol*., *165*, 85–99, 1995.
LaBolle, E. M., G. E. Fogg, and A. F. B. Tompson, Random-walk simulation of transport in heterogenous pourous media: Local mass-conservation problem and implementation methods, *Water Resour. Res*., *32*, 583–593, 1996.
Mantoglou, A., and J. L. Wilson, Simulation of random fields with the turning bands method, *Rep. 264*, 199 pp., Dep. of Civ. Eng., Mass. Inst. of Technol., Cambridge, 1981.
Merz, B., and E. J. Plate, An analysis of the effects of spatial variability of soil and soil moisture on runoff, *Water Resour. Res*., *33*, 2909–2922, 1997.
Prandtl, L., Bericht über Untersuchaungen zur ausgebildeten Turbulenz, *Z. Angew. Math. Mech*., *5*, 136–139, 1925.
Rodríguez-Iturbe, I., Scale of fluctuation of rainfall models, *Water Resour. Res*., *22*, 15S–37S, 1986.
Rodríguez-Iturbe, I., and J. M. Mejía, On the transformation from point rainfall to areal rainfall, *Water Resour. Res*., *10*, 729–735, 1974.
Sánchez-Vila, X., J. Carrera, and J. P. Girardi, Scale effects in transmissivity, *J. Hydrol*., *183*, 1–22, 1996.
Scheibe, T. D., Characterization of the spatial structuring of natural porous media and its impacts on subsurface flow and transport, Ph.D. thesis, Stanford Univ., Stanford, Calif., 1993.
Scheibe, T. D., and D. L. Freyberg, Use of sedimentological information for geometric simulation of natural porous media structure, *Water Resour. Res*., *31*, 3259–3270, 1995.
Sivapalan, M., and G. Blöschl, Transformation of point rainfall to areal rainfall: Intensity-duration-frequency curves, *J. Hydrol*., *204*, 150–167, 1998.
Srivastava, R. M., An annealing procedure for honouring change of support statistics in conditional simulation, in *Quantitative Geology and Geostatistics*, vol. 6, edited by R. Dimitrakopoulos, pp. 277–292, Kluwer Acad., Norwell, Mass., 1994.
Stauffer, D., and A. Aharony, *Introduction to Percolation Theory*, 181 pp., Taylor and Francis, Philadelphia, Pa., 1991.
Taylor, G. I., Diffusion by continuous movements, *Proc. London Math. Soc*., *20*, 196–211, 1921.
Wen, X.-H., and J. J. Gómez-Hernández, Upscaling hydraulic conductivities in heterogeneous media: An overview, *J. Hydrol*., *183*, ix-xxxii, 1996.
Western, A. W., and G. Blöschl, On the spatial scaling of soil moisture, *J. Hydrol*., *217*, 203–224, 1999.
Western, A. W., and R. B. Grayson, The Tarrawarra data set: Soil moisture patterns, soil characteristics and hydrological flux measurements, *Water Resour. Res*., *34*, 2765–2768, 1998.
Western, A. W., and R. B. Grayson, Soil moisture and runoff processes at Tarrawarra, in *Spatial Patterns in Catchment Hydrology—Observations and Modelling*, edited by R. B. Grayson and G. Blöschl, Cambridge Univ. Press, New York, in press, 2000.
Western, A. W., G. Blöschl, and R. B. Grayson, Geostatistical characterisation of soil moisture patterns in the Tarrawarra Catchment, *J. Hydrol*., *205*, 20–37, 1998a.
Western, A. W., G. Blöschl, and R. B. Grayson, How well do indicator variograms capture the spatial connectivity of soil moisture?, *Hydrol. Processes*, *12*, 1851–1868, 1998b.
Western, A. W., R. B. Grayson, G. Blöschl, G. R. Willgoose, and T. A. McMahon, Observed spatial organization of soil moisture and its relation to terrain indices, *Water Resour. Res*., *35*, 797–810, 1999.
Williams, R. E., Comment on "Statistical theory of groundwater flow and transport: Pore to laboratory, laboratory to formation, and formation to regional scale" by G. Dagan, *Water Resour. Res*., *24*, 1197–1200, 1988.

G. Blöschl, Institut für Hydraulik, Technische Universität Wien, Gewässerkunde und Wasserwirtschaft, Karlsplatz 13/223, Vienna A-1040, Austria.

R. B. Grayson and A. W. Western, Cooperative Research Centre for Catchment Hydrology, University of Melbourne, Department of Civil and Environmental Engineering, Parkville, Victoria 3052, Australia.

(Received May 15, 2000; revised July 13, 2000;
accepted August 8, 2000.)